

# In Vivo $^{31}\text{P}$ Solid State MRI of Human Wrists: Short- $T_2$ MRI Using the Scanner $^1\text{H}$ Channel

J. L. Ackerman<sup>1,2</sup>, Y. Wu<sup>2,3</sup>, T. G. Reese<sup>1,2</sup>, H. Cao<sup>2,3</sup>, M. I. Hrovat<sup>4</sup>, S. P. Toddes<sup>5</sup>, and R. A. Lemdiasov<sup>5</sup>

<sup>1</sup>Martinos Center, Department of Radiology, Massachusetts General Hospital, Charlestown, MA, United States, <sup>2</sup>Harvard Medical School, Boston, MA, United States, <sup>3</sup>Department of Orthopedic Surgery, Children's Hospital, Boston, MA, United States, <sup>4</sup>Mirtech, Inc., Brockton, MA, <sup>5</sup>InsightMRI, Inc., Leominster, MA, United States

## Introduction

For accurate MR measurement of bone mineral or matrix density, solid state resonances with extremely short  $T_2$  must be acquired [1-5], necessitating fast electronic recovery of the scanner receiver chain. Current clinical scanner receivers often are not fast enough. In the case of our 3T scanner, the  $^{31}\text{P}$  receiver takes over 200  $\mu\text{s}$  to recover following an RF pulse, completely obliterating any solid state  $^{31}\text{P}$  signal. However, if PIN diode T/R switches are replaced with fast passive diode switches, special preamplifiers are used, and the software receiver recovery delay is reduced, the  $^1\text{H}$  channel recovers in about 5  $\mu\text{s}$  [5]. Therefore, in order to image the mineral content of the wrist by  $^{31}\text{P}$  solid state MRI (SMRI), we constructed a frequency converter that enabled the scanner to operate through its proton channel, while the actual signal excitation and detection occurs at the  $^{31}\text{P}$  frequency. In effect, a special RF "front end" is interposed between the scanner and the  $^{31}\text{P}$  RF coil, enabling high quality  $^{31}\text{P}$  solid state MRI.

## Materials and Methods

In the frequency converter (Figure 1) the high power  $^1\text{H}$  transmit pulse is diverted into a dummy load, and a sample of the pulse is captured via a directional coupler. The pulse sample is mixed with a local oscillator (LO) frequency to yield a  $^{31}\text{P}$  pulse which preserves all the phase and amplitude characteristics of the original  $^1\text{H}$  pulse. The  $^{31}\text{P}$  pulse is amplified by a separate RF power amplifier and applied to the RF coil. The  $^{31}\text{P}$  signal is amplified by a separate low noise preamplifier, mixed back to the  $^1\text{H}$  frequency and directed into the scanner's  $^1\text{H}$  receiver. The RF coil is a 4-strut split T/R birdcage driven in quadrature which fits tightly about the wrist for good filling factor. The T/R switch consists of a quad hybrid and passively switched diode pairs in series with the transmitter and to ground at the preamp. Figure 2 shows the dramatic improvement in receiver recovery provided by the frequency converter. The pulse sequence comprises a 3D radial acquisition of FIDs following a hard RF pulse, with the gradient held constant during the pulse and FID [1,5]. The right or left wrists of 7 healthy volunteers (5 males, 2 females), positioned near isocenter and angled for comfort at 15° horizontal with respect to  $B_0$ , were scanned. The isotropic FOV = 150 mm, matrix  $128^3$ , rectangular excitation pulse 10  $\mu\text{s}$  (10°), dwell 7  $\mu\text{s}$ , gradient 28 mT/m, number of projections 8148, receiver recovery delay 20  $\mu\text{s}$ , TR 275 ms, second acquisition [5] for  $k = 0$  recovery (dwell 20  $\mu\text{s}$ , gradient 7 mT/m, 20 projections), 37 min overall scan time on a Siemens Trio 3T scanner.

## Results and Discussion

The *in vivo* 3T  $^{31}\text{P}$  resonance line width and  $T_1$  of the mineral of the human wrist were found to be 2.0 kHz and 18 s, respectively. Using tubes of hydroxyapatite powder, the spatial resolution was found to be about 5 mm based on the experimentally measured point spread function (including intrinsic spectral resolution and limitations due to the reconstruction). Excellent quality fully isotropic images of the radius and ulna were obtained, with SNR  $\sim$ 30, good enough to enable isosurface contouring to delineate the bone volumes (Figure 3).

## Conclusions

*In vivo*  $^{31}\text{P}$  SMRI visualization of human wrist bone mineral with clinical scanners is feasible with suitable modifications to circumvent the scanners' inherent limitations in reception of short- $T_2$  signals.

## References

1. Wu Y, Chesler DA, Glimcher ML, Garrido L, Wang J, Jiang HJ, Ackerman JL. Multinuclear solid state three dimensional MRI of bone and synthetic calcium phosphates. *Proc Nat Acad Sci USA* 1999; 96: 1574-1578.
2. Robson MD, Gatehouse PD, Bydder GM, Neubauer S. Human imaging of phosphorus in cortical and trabecular bone in vivo. *Magn Reson Med* 2004; 51: 888-892.
3. Anumula S, Magland J, Wehrli SK, Zhang H, Ong H, Song HK, Wehrli FW. Measurement of phosphorus content in normal and osteomalacic rabbit bone by solid-state 3D radial imaging. *Magn Reson Med* 2006; 56: 946-952.
4. Idiyatullin D, Corum C, Park JY, Garwood M. Fast and quiet MRI using a swept radiofrequency. *J Magn Reson* 2006; 181:342-349.
5. Wu Y, Hrovat MI, Ackerman J, Reese TG, Cao H, Ecklund K, Glimcher MJ. Bone matrix imaged *in vivo* by water and fat suppressed proton projection MRI (WASPI) of animal and human subjects. *J Magn Reson Imaging* 2010; 31: 954-963.

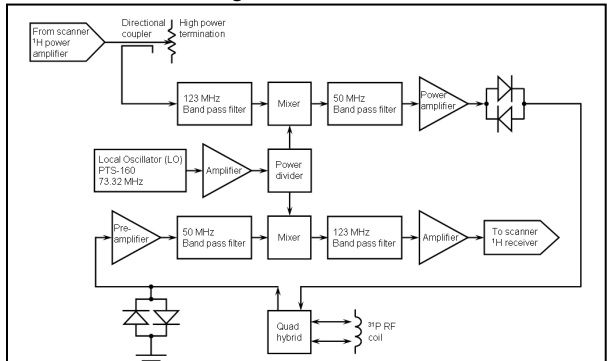


Figure 1. Frequency converter simplified block diagram.

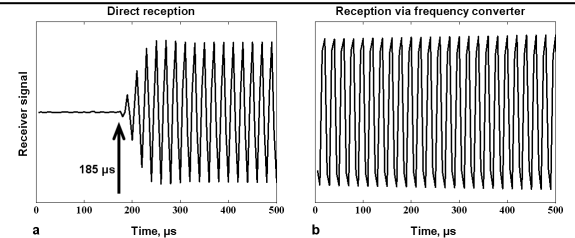


Figure 2. Scanner receiver recovery via direct reception (left) and via frequency converter (right).

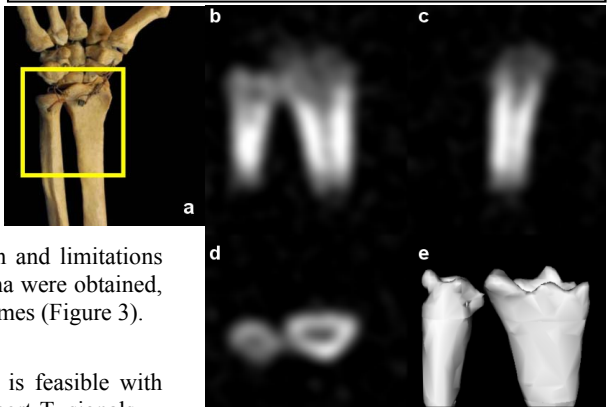


Figure 3. *In vivo*  $^{31}\text{P}$  SMRI of wrist of healthy 41 year old male volunteer. a. Schematic view of scanned region. b-d. Posterior-anterior, lateral, transverse image slices. e. 3D isosurface rendering.